Coastal freshening drives acidification state in Greenland fjords

Henson, Henry; Holding, Johnna M.; Meire, Lorenz; Rysgaard, Søren; Stedmon, Colin; Stuart-Lee, Alice; Bendtsen, Jørgen; Sejr, Mikael

Published in:
Science of the Total Environment

Link to article, DOI:
10.1016/j.scitotenv.2022.158962

Publication date:
2022

Document Version
Publisher's PDF, also known as Version of record

Science of the Total Environment 855 (2023) 158962

Contents lists available at ScienceDirect

Science of the Total Environment

journal homepage: www.elsevier.com/locate/scitotenv

Coastal freshening drives acidification state in Greenland fjords

Henry C. Henson [a,*], Johnna M. Holding [a,b], Lorenz Meire [c,d], Søren Rysgaard [a], Colin A. Stedmon [e], Alice Stuart-Lee [c], Jørgen Bendtsen [f], Mikael Sejr [a,b]

[a] Arctic Research Centre, Aarhus University, Denmark
[b] Department of Ecoscience, Aarhus University, Denmark
[c] Department of Estuarine and Delta Systems, Royal Netherlands Institute for Sea Research, Yerseke, the Netherlands
[d] Greenland Climate Research Centre, Greenland Institute of Natural Resources, Nuuk, Greenland
[e] National Institute of Aquatic Resources, Technical University of Denmark, Lyngby, Denmark
[f] Globe Institute, University of Copenhagen, Copenhagen, Denmark

HIGHLIGHTS

- Greenland fjords provide an outlook for a future, fresher, Arctic coastal Ocean.
- Calcium carbonate corrosive conditions are found surrounding Greenland.
- Deep water corrosivity was driven by accumulation of CO_2 from remineralization.
- Surface corrosivity was caused by alkalinity dilution from glacial meltwater.
- Greenland Ice Sheet melting will increase already present corrosive conditions.

GRAPHICAL ABSTRACT

Conceptual diagram of the coastal biogeochemical variation driving aragonite saturation state in West and East Greenland (left). Local variation on a fjord scale is controlled by circulation driven by glacial morphology (land terminating glacier vs marine terminating glacier) (right).

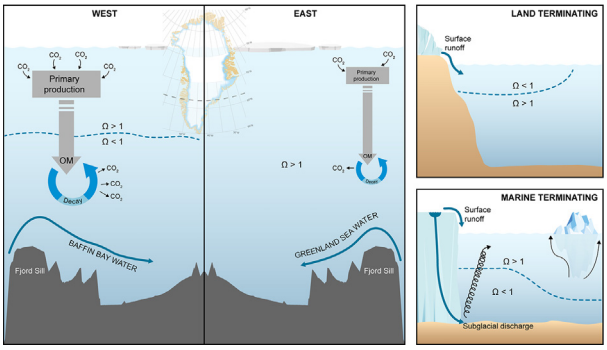

ARTICLE INFO

Editor: Martin Drews

Keywords:
Ocean acidification
Arctic
Climate change
Carbonate saturation state
Seawater chemistry
Freshening
Greenland fjord
Carbon dioxide
Biological pump
CO_2

ABSTRACT

Greenland's fjords and coastal waters are highly productive and sustain important fisheries. However, retreating glaciers and increasing meltwater are changing fjord circulation and biogeochemistry, which may threaten future productivity. The freshening of Greenland fjords caused by unprecedented melting of the Greenland Ice Sheet may alter carbonate chemistry in coastal waters, influencing CO_2 uptake and causing biological consequences from acidification. However, few studies to date explore the current acidification state in Greenland coastal waters. Here we present the first-ever large-scale measurements of carbonate system parameters in 16 Greenlandic fjords and seek to identify the drivers of acidification state in these freshening ecosystems. Aragonite saturation state (Ω), a proxy for ocean acidification, was calculated from dissolved inorganic carbon (DIC) and total alkalinity from fjords along the east and west coast of Greenland spanning 68–75°N. Aragonite saturation was primarily >1 in the surface mixed layer. However, undersaturated—or corrosive—conditions (Ω < 1) were observed on both coasts (west: Ω = 0.28–3.11, east: Ω = 0.70–3.07), albeit at different depths. West Greenland fjords were largely corrosive at depth while undersaturation in East Greenland fjords was only observed in surface waters. This reflects a difference in the coastal boundary conditions and mechanisms driving acidification state. We suggest that advection of Sub Polar Mode Water and accumulation of DIC from organic matter decomposition drive corrosive conditions in the West, while freshwater alkalinity dilution drives acidification in the East. The presence of marine terminating glaciers also impacted local acidification

* Corresponding author.
E-mail address: henrychenson@gmail.com (H.C. Henson).

http://dx.doi.org/10.1016/j.scitotenv.2022.158962
Received 28 July 2022Accepted 19 September 2022
Available online 26 September 2022

states by influencing fjord circulation: upwelling driven by subglacial discharge brought corrosive bottom waters to shallower depths. Meanwhile, discharge from land terminating glaciers strengthened stratification and diluted alkalinity. Regardless of the drivers in each system, increasing freshwater discharge will likely lower carbonate saturation states and impact biotic and abiotic carbon uptake in the future.

1. Introduction

Global oceans have slowed the accumulation of greenhouse gasses in the atmosphere by absorbing roughly one third of all anthropogenic produced carbon dioxide (CO_2) (Sabine, 2004). However, dissolution of CO_2 has consequences by altering seawater carbonate chemistry. Dissolved CO_2 reacts with water forming carbonic acid (H_2CO_3) and driving a reduction in pH, a process known as ocean acidification. Acidification has significant consequences for ecosystem productivity and marine food webs, including culturally and economically valuable fisheries. At particular risk is calcium carbonate ($CaCO_3$) producing organisms. When the saturation state (Ω) of $CaCO_3$ is below 1, $CaCO_3$ is prone to chemical dissolution, however $CaCO_3$ production becomes energetically costly for marine calcifiers before this (Doney et al., 2009; Feely, 2004). For example, one key species of the Arctic food web, zooplankton *Limacina helicina*, has reduction of shell calcification at Ω below 1.4 (Bednaršek et al., 2012, 2019). Additionally, ocean acidification impacts metabolic reactions (Guinotte and Fabry, 2008) and may therefore affect all levels of the trophic system. Yet, ocean acidification does not threaten all ocean basins equally. High freshwater inputs, cold waters, and diminishing yearly sea ice cover make the Arctic particularly susceptible to CO_2 uptake and consequent ocean acidification (AMAP, 2018). Model simulations predict the Arctic Ocean will be the first basin to develop wide-scale acidification and carbonate corrosivity (Steinacher et al., 2009; Terhaar et al., 2020).

Coastal Arctic waters are of particular interest as they are the most affected by freshwater runoff. Coastal freshening can enhance stratification and change circulation (Carmack et al., 2016), particularly for seawater constrained within fjords. In Greenlandic coastal waters, fjords function as biogeochemical gateways between the Greenland ice sheet and the open ocean, providing insight on the potential impact of freshening in the Arctic. Acidification in coastal Greenland is complex in part due to the interplay between various boundary conditions and biological processes. Three significant boundaries influence the biogeochemistry within these transition corridors: the air-sea interface where atmospheric CO_2 is exchanged, the mixing between fjord and shelf water masses, and the land-sea interface where major quantities of freshwater are discharged. Contemporaneously, biological production and remineralization also shape carbon dynamics by removing or adding CO_2 to the system.

Dissolved CO_2 can lead to acidification in both surface and deep waters. Surface water dissolved inorganic carbon (DIC) levels are the result of air-sea CO_2 exchange, physical mixing and heterotrophic and autotrophic activity. Increasing atmospheric CO_2 concentrations elevates surface DIC while driving carbonate ion consumption and a reduction in Ω (Qi et al., 2022). Meanwhile, photosynthesis removes DIC from sunlit waters causing the reverse effect (Bates and Mathis, 2009). Accumulation of deep water DIC results from the decomposition and respiration (remineralization) of organic matter that sinks from productive arctic surface waters. This respired CO_2 accumulates in deep waters (Bates et al., 2014) and tends to reduce in Ω and pH as the water mass ages.

Shelf water masses have inherently different Ω baselines which, when mixed, alter fjord carbon dynamics. The East Greenland Current brings cold and fresh water from the Arctic Ocean (Aagaard and Coachman, 1968). Meanwhile western Greenland fjords output into the Labrador Sea, Davis Strait and Baffin Bay. Water masses in West Greenland consist of warm SubPolar Mode Water (SPMW), cold Baffin Bay Polar Mode Water (BBPW) and West Greenland coastal water (CW) (Rysgaard et al., 2020). Inflow of Pacific water masses, which are low in Ω due to global circulation history and their time spent in the freshening Beaufort Gyre, act to lower saturation states as they pass through the Fram Strait, Nares Strait or Canadian Archipelago (Sutherland et al., 2009; Yamamoto-Kawai et al., 2013). However, shelf water's impacts on fjord waters are constrained by fjord specific conditions e.g. bathymetry, sill depth, estuarine circulation, subglacial circulation, dense coastal inflows and intermediate baroclinic circulation (Mortensen et al., 2011). Additionally, fjord stratification and circulation are determined in part by glacial morphology. Marine-terminating glaciers and land-terminating glaciers release meltwater at different depths with differing consequences on biogeochemistry and circulation (Meire et al., 2017). Yet, these differences have to be linked to patterns in ocean acidification (Cantoni et al., 2020; Ericson et al., 2019; Evans et al., 2014; Fransson et al., 2020) as multi-fjord studies are uncommon.

Regardless of shelf water masses and fjord morphology, the impact of ocean acidification on the carbonate system is determined by the buffering capacity of seawater. Hence, carbonate chemistry is dependent on the amount and source of freshwater input. River and glacial runoff are typically low in both alkalinity and carbonate ions relative to marine waters (Brown et al., 2020; Chierici and Fransson, 2009; Evans et al., 2014; Fransson et al., 2015; Mathis et al., 2011; Yamamoto-Kawai et al., 2013). Thus, freshwater input dilutes seawater alkalinity and DIC, lowering the capacity of seawater to resist changes in pH from uptake of atmospheric CO_2 (Azetsu-Scott et al., 2014; Cantoni et al., 2020; Chierici and Fransson, 2009; Evans et al., 2014; Fransson et al., 2013, 2020; Robbins et al., 2013). The coastal area of Greenland is strongly influenced by a variety of freshwater sources such as runoff from precipitation and snowmelt, glacial meltwater, and sea ice melt. The amount of meltwater runoff is accelerating each year and the annual mass loss from the Greenland Ice Sheet has increased 6-fold since the 1980s (Mouginot et al., 2019) heightening the risk for (future) surface acidification.

Buildup of DIC in shelf waters has already been observed to cause aragonite undersaturation, conditions that are corrosive to carbonate, in the Bering (Mathis et al., 2011), Chukchi (Bates et al., 2009), Beaufort (Mathis et al., 2012; Zhang et al., 2020) and East Siberian (Anderson et al., 2011) seas, as well as the Canadian Archipelago (CAA) (Yamamoto-Kawai et al., 2013), and Hudson Bay (Azetsu-Scott et al., 2014). Meanwhile, surface water aragonite undersaturation has also been observed in the CAA (Chierici and Fransson, 2009), Beaufort Sea (Chierici and Fransson, 2009; Mathis et al., 2012), Hudson Bay (Azetsu-Scott et al., 2014), Gulf of Alaska (Evans et al., 2014), the Siberian Shelf (Anderson et al., 2011), and near undersaturation in Svalbard fjords (Cantoni et al., 2020). However, to date, aragonite saturation as well as its drivers have not been evaluated in Greenland Fjords.

Here we present data from two coastal Greenland cruises covering a large range of both marine and land terminating glacial fjords, in North-East and West Greenland spanning ~6° of latitude (Fig. 1). Often these biogeochemically complex systems are only studied in one fjord system and therefore do not examine drivers in variable conditions. This study establishes the first measurements of aragonite saturation state in several Greenland fjords and takes a first step toward assessing the drivers of Ω. This larger spatial coverage allows us to better understand the factors affecting aragonite saturation in coastal Greenland waters.

2. Methods

2.1. Survey description

Data was collected during two research cruises in Greenland. One cruise was conducted with RV Sanna (69–75°N) during 12–30 August 2016 in West Greenland, and a second in East Greenland with HDMS Lauge Koch (68–74°N) between July 30 and August 24, 2018 (Fig. 1). Additional stations in Young Sound, East Greenland were sampled in 2018 as part of the Greenland Ecosystem Monitoring (Christensen et al., 2017).

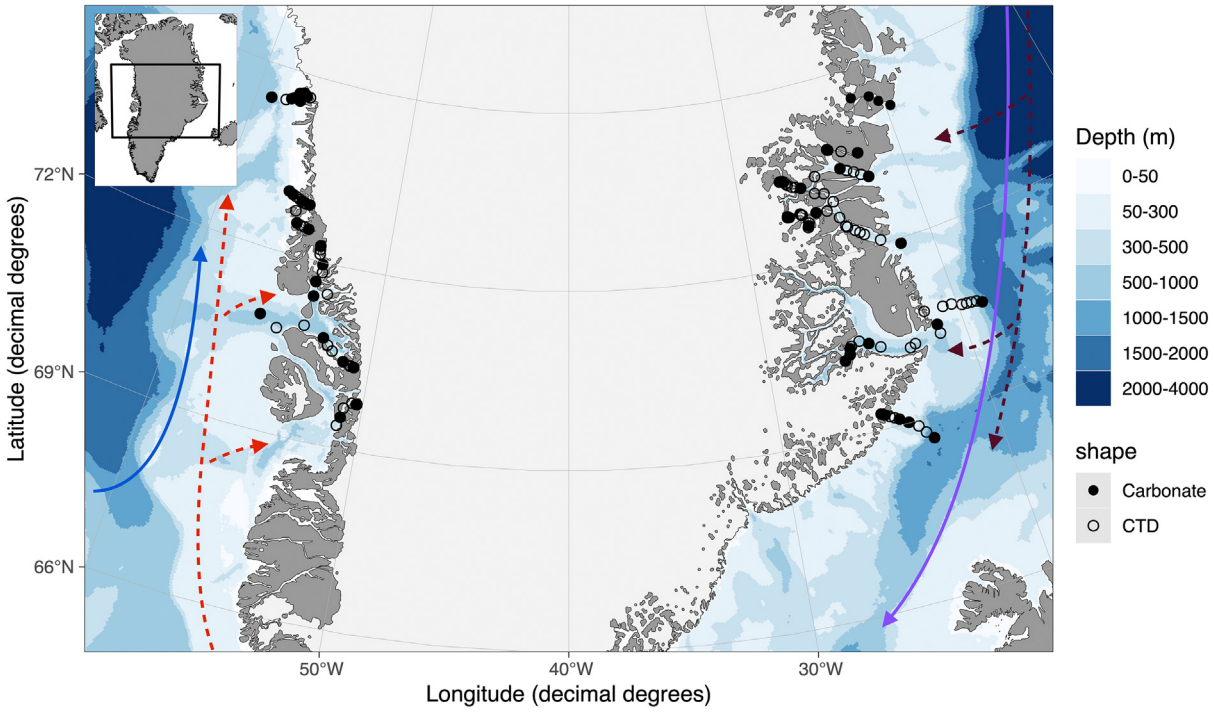

Fig. 1. Map of Greenland illustrating the distribution of the 145 CTD profiles (open circles) and 52 carbonate chemistry sample sites (filled circles). Arrows depict movement of major water masses. (Blue: Baffin Bay Polar Water, Red: Deep Subpolar Mode Water, Purple: Arctic Ocean Outflow, Maroon: Atlantic Water).

2.2. Environmental sampling

A CTD (Seabird19 + V2 and Seabird SBE25 on West coast and East coast cruises respectively) was used to measured conductivity, temperature, and pressure. All salinity values are reported as practical salinity (S_p) hereafter referred to as S. Additional sensors recorded chlorophyll-a fluorescence, photosynthetically available radiation (PAR), and dissolved oxygen (Bendtsen et al., 2017; Carlson et al., 2020; Holding et al., 2021).

Water samples for dissolved inorganic carbon (DIC), total alkalinity (TA), dissolved oxygen, and $\delta^{18}O$-H_2O were collected from Niskin bottles. Samples for oxygen concentration were taken at least once for each cruise and were analyzed using Winkler titration. The results were used to calibrate the oxygen sensors on the CTD instruments. Water samples for DIC and TA determination were transferred directly from the Niskin bottle into triplicate 12 ml exetainers with a gas tight Tygon tubes, allowing overflow of at least 3 times the volume of the exetainer. Triplicate exetainers were collected for both DIC and TA at each depth. Samples were preserved with $HgCl_2$ (saturated solution) to a final concentration of 0.02 %. TA was measured on an Apollo SciTech AS-ALK2 total alkalinity titrator based on the Gran titration procedure for samples in West Greenland. Samples for East Greenland were measured on automatic titrator (Metrohm 888 Titrando), and a combined Metrohm glass electrode (Unitrode). DIC samples were analyzed on Apollo SciTech's AS-C3 analyzer for both cruises, using a sample volume of 0.5 ml. Routine analysis of Certified Reference Materials (provided by A. G. Dickson, Scripps Institution of Oceanography) verified that the accuracy of DIC and TA measurements. The average standard deviation for the triplicate DIC measurements was 8.16 and 2.68 μmol kg^{-1} for East and West Greenland respectively. Meanwhile, triplicate TA measurements had mean standard deviation values of 13.38 and 9.29 μmol kg^{-1} for East and West Greenland respectively. Eastern TA/DIC values had higher triplicate standard deviations than the western cruise, so we removed outliers in triplicate samples following the rule of 1*IQR of log(coefficient of variance).

The western cruise included 56 CTD casts with 23 stations analyzed for carbonate chemistry. Meanwhile the eastern cruise took 89 CTD casts with 29 of the stations including carbonate chemistry analysis. Fjord transects were assigned glacial type based on the dominant glacial output (marine- or land-terminating) present within each fjord by visual inspection of satellite imagery.

The $\delta^{18}O$ isotopic compositions of the water samples were analyzed with a Cavity Ringdown Spectrometer, L2130-i Isotopic H20 (Picarro Inc., USA). Six injections were taken from each sample and three were excluded to remove any residual results from the previous sample. Vapor content, $\delta^{18}O$ values were calculated relative to standards. Four standards were measured at the beginning and end of the sample set. The external standards used to calibrate the results were Vienna Standard Ocean Water 2 (VSMOW2), Greenland Summit Precipitation (GRESP) and Standard Light Antarctic Precipitation 2 (SLAP2).

2.3. Carbonate chemistry analysis

Marine calcifiers rely on availability of carbonate ions to build $CaCO_3$ shells and skeletons. In this study, the saturation state of aragonite Ω_{arg} (hereafter Ω) was used as a proxy for ocean acidification because the $CaCO_3$ polymorph aragonite dissolves more easily than calcite, the other major form of $CaCO_3$ used by marine organisms. The saturation state of aragonite therefore represents the frontline of the effect of acidification on biological communities. Seawater carbonate system parameters, including the saturation state of aragonite (Ω) and pH were calculated from DIC and TA using the R package Seacarb (Lavigne and Gattuso, 2010). No equilibrium constants (K1 and K2) currently fit all the salinity and temperature conditions of this dataset, so constants from Mehrbach et al. (1973), as refit by Dickson and Millero (1987) and Lueker et al. (2000), were used for best cross-comparison between studies. Although some uncertainty is introduced in this calculation, Leuker et al. (2000) constants were the most internally consistent and expected to be applicable to most near-surface ocean conditions (Woosley, 2021). Two samples at 400 and 1000 m on the east coast did not have corresponding temperature and salinity (TS) data. In order to better understand Ω at depth on the East coast, historical TS data from the shelf outside the fjords was averaged at 400 and 1000 m to supply necessary data for Ω calculation (Key et al., 2015). TS data was not expected to change greatly as these depths are below the pycnocline. While this introduces some error into these two datapoints, this calculation allows for the valuable comparison of deep water between the two coasts.

Table 1
Coastal Greenland water mass salinity and $\delta^{18}O$ endmember values from the literature.

Water mass	Salinity (PSU)	$\delta^{18}O$ (‰)	Source
Greenland glacial meltwater	0	−26.9 ± (3.1)	Carlson et al. (2019)
Sea ice meltwater	3.8 ± (0.45)	−0.6 ± (1.6)	Forryan et al. (2019)[a]
Atlantic Water	34.89 ± (0.09)	0.28 ± (0.06)	Forryan et al. (2019)[a]
Polar Mode Water	32.14	−2.23	This study
Baffin Bay Polar Water	33.58	−0.81	This study

[a] Mean values from 5 separate Arctic studies.

2.4. Freshening analysis

Source water fractions (F) of sea ice meltwater, glacial meltwater, and seawater were estimated using salinity (S) and $\delta^{18}O$ endmember values in the following mass balance calculation (Azetsu-Scott et al., 2014; Cox et al., 2010; Yamamoto-Kawai et al., 2008)

$$F_{SIM} + F_{GM} + F_{SW} = 1 \quad (1)$$

$$S_{sample} = S_{SIM} \times F_{SIM} + S_{GM} \times F_{GM} + S_{SW} \times F_{SW} \quad (2)$$

$$\delta^{18}O_{sample} = \delta^{18}O_{SIM} \times F_{SIM} + \delta^{18}O_{GM} \times F_{GM} + \delta^{18}O_{SW} \times F_{SW} \quad (3)$$

where the subscripts SIM, GM, and SW represent the sample water parcels sea ice meltwater, glacial meltwater, and seawater, respectively. The salinity and $\delta^{18}O$ endmember values are detailed in Table 1. For source water fraction calculations, Greenland glacial meltwater was used as the endmember for meteoric water as glacial melt is the main runoff input in these fjord and coastal systems. In addition, Polar Mode Water (PMW) and Baffin Bay Polar Water (BBPW) endmembers were used for seawater fractions on East and West coasts respectively. Endmembers for PMW and BBPW were identified using samples from the shelf slope with the lowest temperature at depths above 200 m.

3. Results

3.1. Hydrography

Sampling on the east coast of Greenland included several stations on the shelf while in west Greenland, sampling was primarily located inside the fjords. Hydrographic conditions in East Greenland showed a slightly larger salinity range compared to the west coast (16.02–34.92 vs. 19.76–34.53) (Fig. 2a). However, both coasts showed comparable temperature ranges (Fig. 2b). Western samples were collected in 4 fjords dominated by marine-terminating glaciers (MTGs), 2 fjords with land-terminating glaciers (LTGs) and 1 ambiguous fjord (no glacial output). Meanwhile eastern analyses were conducted in 3 fjords with dominant MTGs, 3 fjords with a LTG output and 3 ambiguous fjords/shelf transects.

3.2. Carbonate saturation

Mean dissolved inorganic carbon (DIC) was significantly elevated ($p < 0.05$) at every depth >20 m in western samples compared to eastern stations (Fig. 2e). Meanwhile, total alkalinity (TA) was more variable in east stations (Fig. 2f) reaching both more diluted values in the surface

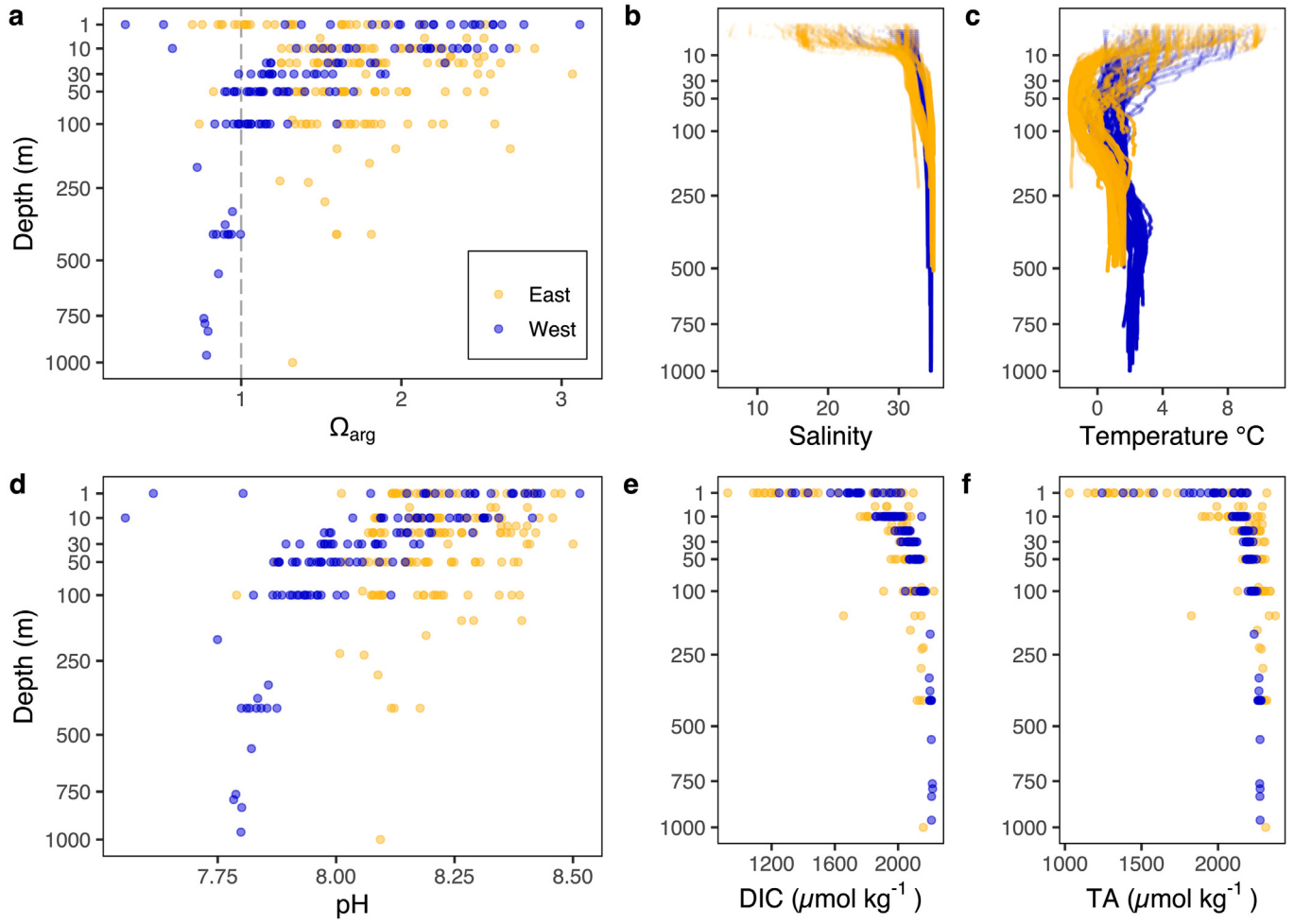

Fig. 2. Calculated aragonite saturation state (a) and pH (d), as well as measured salinity (b), temperature (c), DIC (e), and TA (f) profiles.

layer and significantly elevated concentrations below 20 m with respect to western stations.

Saturation states (Ω) and pH levels for stations in west Greenland reached consistently lower levels compared to east Greenland (Fig. 2a, c), especially at depth. A significant difference in means was observed between Ω of East and West Greenland at all depths except 10–20 m. Eastern surface samples were lower than western surface samples with several instances of corrosive conditions (East Ω μ = 1.34, West Ω μ = 2.05, $p < 0.01$). However, by 30 m this trend was reversed with western stations having lower Ω (East Ω μ = 2.47, West Ω μ = 1.34, $p < 0.05$). At 100 m one third of all western measurements showed aragonite undersaturation while only one eastern sample was undersaturated (East Ω μ = 1.70, West Ω μ = 1.08, $p < 0.001$). Moreover, below 100 m all western samples and no eastern samples exhibited corrosive conditions. However, it should be noted that fewer samples were taken at depth in eastern fjords, and only one was taken below 400 m. Corrosive conditions as shallow as ~40 m in west Greenland indicate unique mechanisms occurring in fjords as the saturation horizon in Baffin Bay and the Davis Strait is between 200 and 700 m (Azetsu-Scott et al., 2010; Yamamoto-Kawai et al., 2013).

3.3. Drivers of aragonite saturation

Fig. 3 illustrates the main drivers of aragonite saturation state. Apparent Oxygen Utilization (AOU), also known as deviation from O_2 saturation, is an indication of biological activity with positive values signifying bacterial O_2 consumption. Meanwhile negative AOU values are indicative of photosynthetic O_2 production as they are seen concurrently with nitrate (NO_3) and DIC drawdown (Supplemental Fig. 1a). Furthermore, TA describes the capacity of seawater to buffer acidity change. Within western surface layer samples (<40 m), primary production's consumption of CO_2 resulted in elevated Ω levels (Fig. 3a) while diverse TA concentrations drove Ω variability (Fig. 3b). Below 40 m, corrosive conditions were driven by respiration of organic matter and the resultant production and accumulation of CO_2 in western waters (Fig. 3a). East Greenland illustrated a weaker relationship between AOU and Ω (Fig. 3a). The saturation state of the east Greenland surface layer was instead controlled by dilution of alkalinity (Fig. 3b).

3.4. Freshening effects

Dilution of alkalinity in the surface layer resulted from the runoff or input of meltwater (Fig. 4a). As total freshwater fractions increased, more corrosive conditions were observed (Fig. 4b). The relationships between salinity and $\delta^{18}O$ are shown in Fig. 5 along with the literature endmembers listed in Table 1. By connecting water mass endmembers within a salinity-$\delta^{18}O$ space we can create a mixing diagram where mixing between water mass properties causes measured water parcels to lie along lines connecting core water masses (Forryan et al., 2019). Fig. 5 illustrates that our samples mainly involve a mixture of seawater and glacial meltwater input. However, it appears that low salinity values on the east coast have elevated $\delta^{18}O$ values that suggest a greater impact of sea ice and sea ice melt in these surface waters. Mass balance studies of freshwater show that melt from the Greenland ice sheet only makes up ~10 % of freshwater in East Greenland Current waters compared with freshwater from the Arctic Ocean (Bamber et al., 2018). Still, within fjord systems in this study, the dominant source of freshwater was meltwater from the Greenland ice sheet in addition to sea ice melt (Fig. 4c, d) with the largest fractions being in the upper 5 m.

Glacial and sea ice meltwater had varying effects of alkalinity dilution and therefore Ω reduction. In both east and west Greenland, increasing glacial meltwater fractions were more correlated to TA dilution (Fig. 4c) than sea ice melt (Fig. 4d). On the east coast, sea ice meltwater contributed to alkalinity dilution. However, western samples did not display the same trend. Negative F_{SIM} may suggest the influence of sea ice formation (Dodd et al., 2012) could also be associated with reduced TA. However, overall west Greenland had a small influence from sea ice.

3.5. Circulation-driven glacial effects

Distribution of corrosive conditions in fjords also appears to be influenced by glacier type. Glacial meltwater enters the fjord waters at different depths depending on whether a fjord is impacted by marine- and/or land-terminating glaciers (MTGs and LTGs respectively). River surface runoff from LTGs led to a warmer, fresher surface lens where corrosive surface conditions can be observed (Table 2). Meanwhile, in fjords with MTGs, corrosive conditions were less likely to be observed on the surface and were instead often seen at greater depths coincident with remineralized water with elevated AOU. However, corrosive water was often present at shallower depths close to the MTG terminus compared to in the outer fjord (Supplemental Fig. 2).

3.6. Link to hydrographic conditions

The baseline level of aragonite saturation inside a fjord also depends on the water masses surrounding coastal Greenland. In West Greenland water masses are made up of subpolar mode water (SPMW), Greenland Coastal

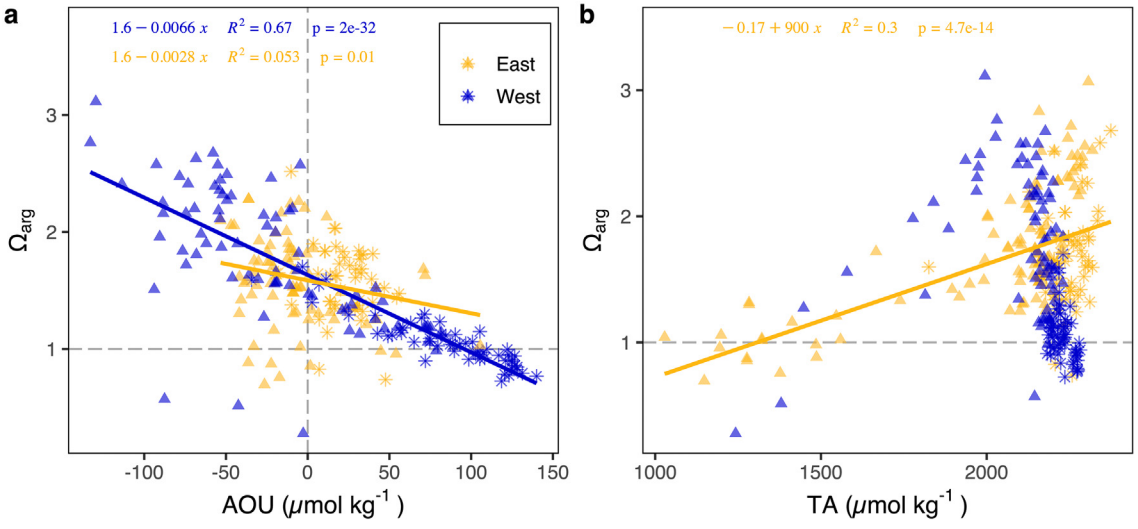

Fig. 3. Relationships between Ω and Apparent Oxygen Utilization (AOU) (a) and Ω and TA (b) for the East and West coasts. Triangle points are samples above 40 m while star symbols illustrate samples taken deeper than 40 m.

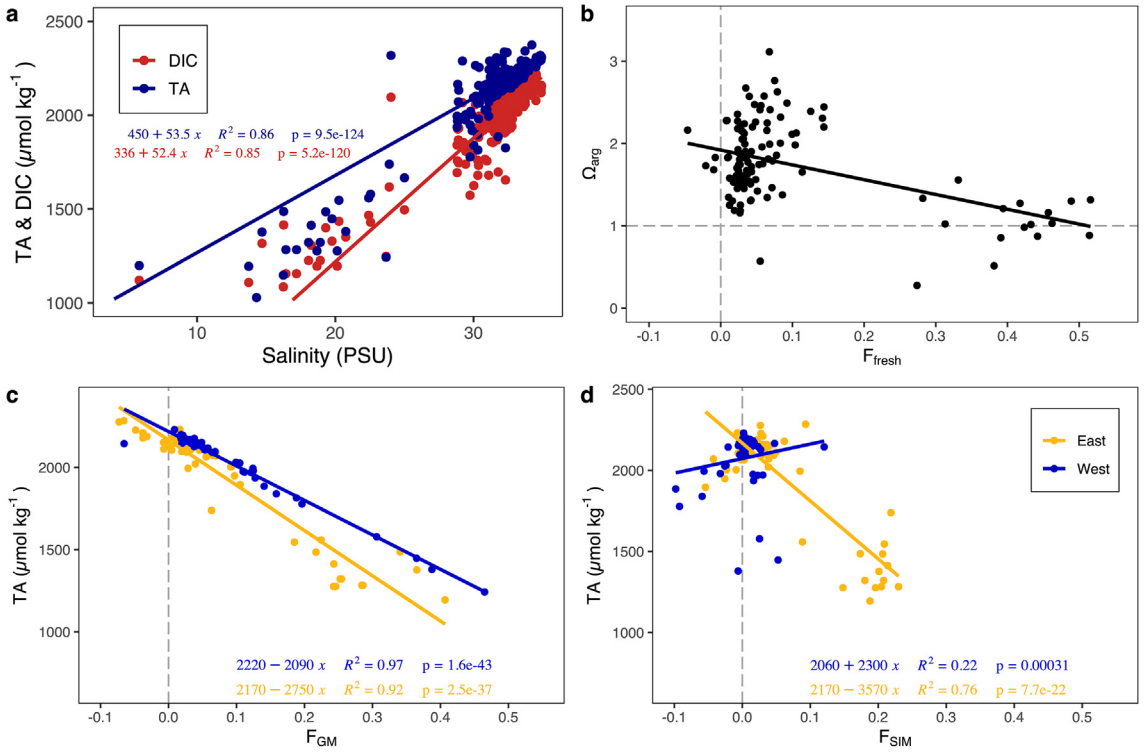

Fig. 4. Measurements of DIC and TA as a function of salinity (a). Panels b–d illustrate influence of freshwater in the surface layer (<25 m). Aragonite saturation state (Ω) decreased with freshwater fraction (F_{fresh}) for all surface water samples (b). Relationships of TA and glacial meltwater fractions (F_{GM}) as well as TA and fraction of sea ice melt (F_{SIM}) are also illustrated for eastern and western cruise data (c, d).

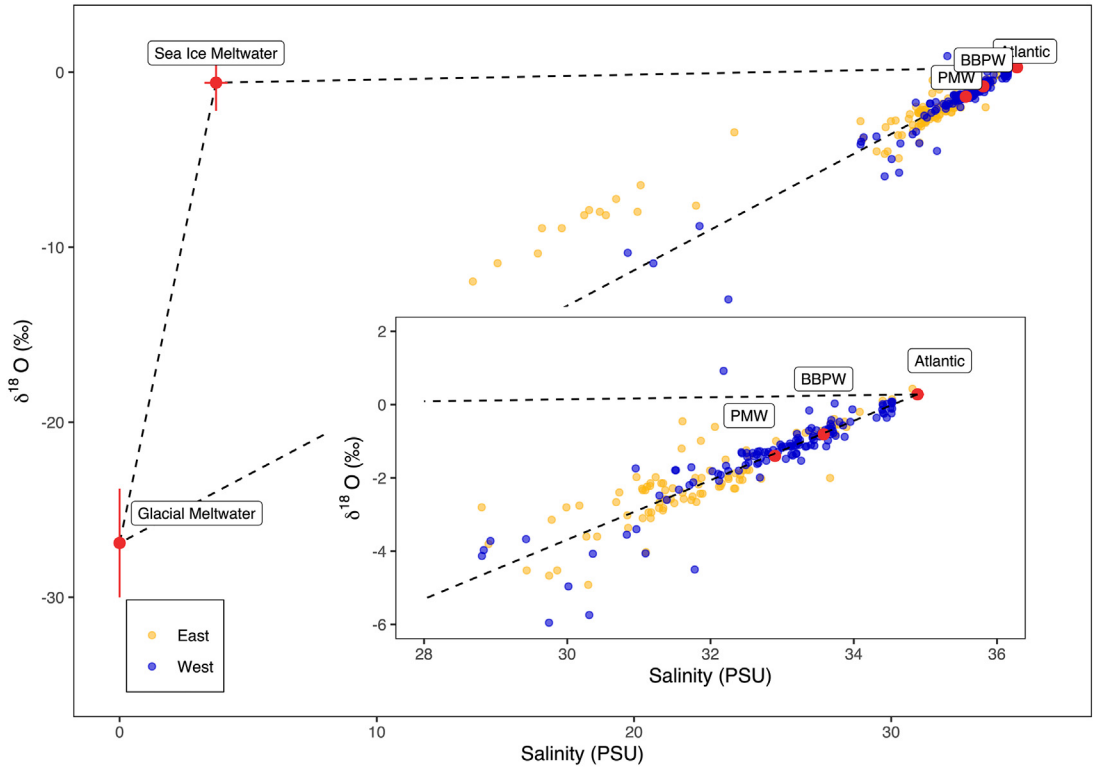

Fig. 5. Salinity – $\delta^{18}O$ relationships for all samples, with literature endmembers ± (sd) marked in red. Black dashed lines represent mixing lines between endmembers (a).

Table 2
Median ± (SD) values for hydrographic and carbonate parameters at 1 m depth within 40 km from innermost station in fjords with marine-terminating (MTG) and land-terminating glaciers (LTG).

Variable	MTG	LTG	[a]	Units
Salinity	29.9 ± (4.1)	20.7 ± (8.2)	*	PSU
Temperature	3.16 ± (1.7)	7.97 ± (1.9)	***	°C
Ω_{arg}	2.22 ± (0.7)	1.04 ± (0.6)	**	
TA	1977 ± (254)	1380 ± (282)	**	μmol kg^{-1}
DIC	1735 ± (213)	1350 ± (247)	**	μmol kg^{-1}
	n stations = 14	n stations = 7		

[a] Significance codes: '***' 0.001 '**' 0.01 '*' 0.05.

Water (CW) and Baffin Bay Polar Water (BBPW) (Fig. 6a). Meanwhile, east Greenland water masses are a mix of Atlantic Water (AW), Lower Halocline Water (LHW), and Polar Mode Water (PMW) (Fig. 6b). The most corrosive conditions observed on the west coast were comprised of deep Subpolar Mode Water which is advected into western fjords from the Greenland Shelf (Rysgaard et al., 2020). Corrosive conditions on the East Coast are found only in the freshest surface waters.

4. Discussion

4.1. State of Greenland fjord acidification

Corrosive conditions were observed in both East and West Greenland fjords, yet at shallower depths than in surrounding seas (Azetsu-Scott et al., 2010; Fransner et al., 2020; Yamamoto-Kawai et al., 2013). On the West coast, an aragonite saturation horizon developed in every fjord visited. These horizons were as shallow as ~40 m depth with all samples below 100 m exhibiting undersaturated conditions. In contrast, eastern fjords did not appear to develop a saturation horizon, though we only have 1 data point from below 400 m. Studies on the East Greenland Shelf and Greenland Sea suggest that the saturation horizon may begin around 1000 m (Fransner et al., 2020; Olafsson et al., 2009), such that we would not expect these undersaturated water masses to reach the NE Greenland shelf or fjords. Buildup of DIC in bottom water observed only in western fjords may reflect higher productivity and subsequent sinking flux and mineralization in deeper fjords or a distinct shelf water mass which has been advected into the fjord (Fig. 7). While eastern fjords did not display corrosive waters at depth, extensive surface undersaturation was observed close to glacial outputs. This emphasizes the importance of coastal freshening and the influence of glacial run-off, as surface undersaturation has not been observed in Baffin Bay, the Labrador Sea, Fram Strait, Greenland Sea, or Iceland Sea (Azetsu-Scott et al., 2010; Chierici and Fransson, 2009; Fransner et al., 2020; Yamamoto-Kawai et al., 2013). Moreover, even other Atlantic/Arctic fjord systems such as Svalbard have not displayed surface corrosivity to date (Cantoni et al., 2020; Fransson et al., 2015; Jones et al., 2021) highlighting the unique circumstances in coastal Greenland. The nearest prevalence of surface undersaturation occurs in Hudson Bay and the Laptev Sea due to fluvial TA dilution and terrestrial organic matter remineralization respectively (Azetsu-Scott et al., 2014; AMAP, 2018) as well as in Alaska due to glacial melt (Evans et al., 2014). Regardless, when comparing both coasts in this study, divergent placement of corrosivity in surface waters and deep waters exposes several different mechanisms working in tandem to drive low saturation states around Greenland.

4.2. Biological remineralization drives DIC buildup in productive fjords

Biological activity has a large impact on dissolved inorganic carbon concentrations in the water column. Primary production in surface waters removes DIC from seawater while bacterial decomposition is a source of DIC. Concurrent elevated AOU in deeper water (>40 m on the West Coast) indicates there is a greater bacterial oxygen utilization, resulting in the buildup of CO_2 that causes the observed lower aragonite saturation state. Model and satellite ocean color observations show higher productivity on the western coast of Greenland in our study area (west: 49.5 ± 13.89 vs. east: 23.6 ± 7.12 g C m^{-2} yr^{-1}) (Vernet et al., 2021). Within our study, western coast photic zone oxygen production appears to support these findings (Fig. 3a). This highlights the ability of primary producers to alleviate acidification in summer, something that has also been shown to occur in other Greenland fjords (Krause-Jensen et al., 2015). There is also evidence of benthic-pelagic coupling following high production in West Greenland coastal waters. Where there are greater levels of primary productivity, there will be elevated levels of particulate organic matter that sinks below the photic zone where it can be mineralized. However, the relative influence of the biological pump and shelf water advection on Ω are unknown. In western waters, copepod production was observed only being able to graze down a fraction of phytoplankton biomass leaving large quantities of organic matter to be exported below the photic zone (Arendt et al., 2010). Excess organic matter will further fuel bacterial activity and contribute to establishing corrosive conditions at depth. Meanwhile, within the photic zone, primary production may act to mitigate acidification. Greenland's eastern coast had oxygen levels closer to saturation throughout the water column suggesting that there is both less primary production in the photic layer and less remineralization at depth (Middelbo et al., 2018). This is potentially because of a lower sinking organic matter flux,

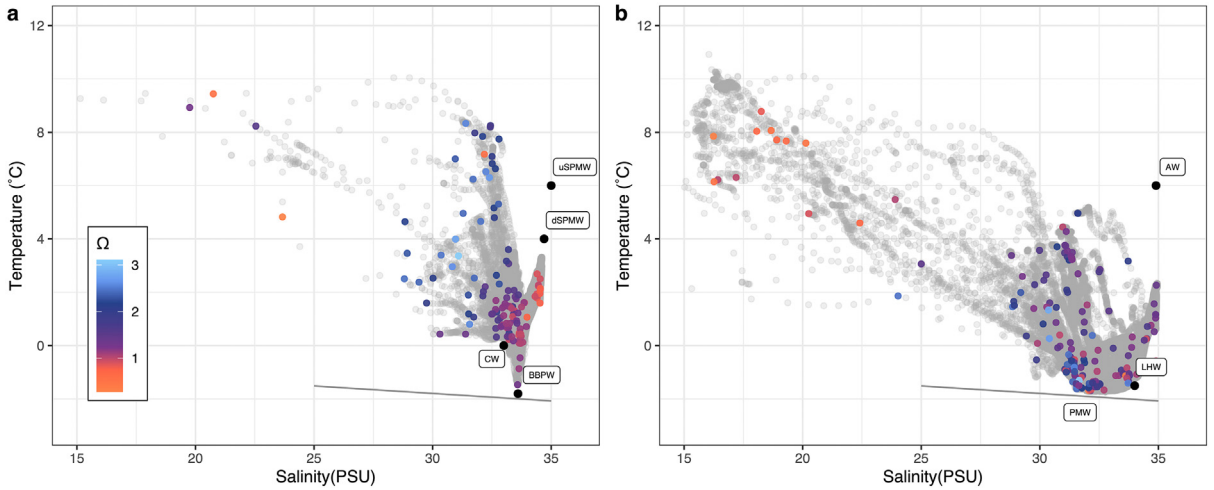

Fig. 6. West coast (a) and east coast (b) temperature-salinity plots. Abbreviations represent water types of upper and deep Sub Polar Mode Water (uSPMW and dSPMW, sensu (Rysgaard et al., 2020)), West Greenland Coastal Water (CW), Baffin Bay Polar Water (BBPW), Atlantic Water (AW), Lower Halocline Water (LHW, Bourke et al., 1987; Willcox et al., n.d.) and Polar Mode Water (PMW). The grey freezing line is also depicted.

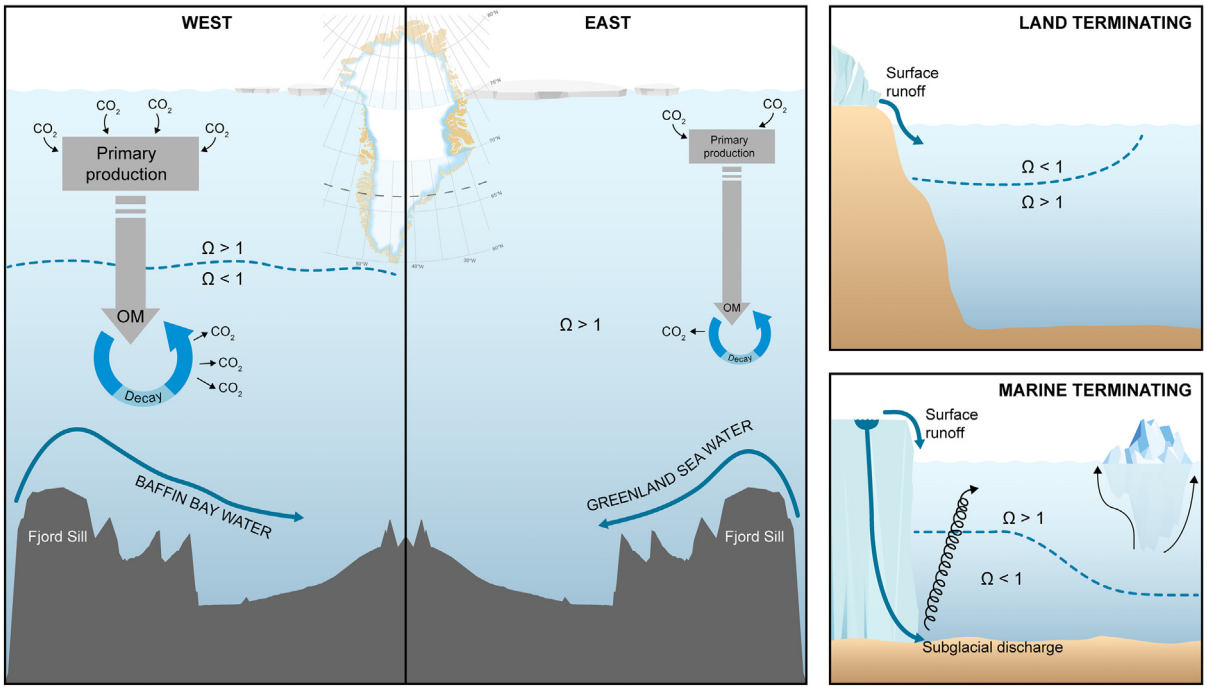

Fig. 7. Conceptual diagram of the coastal biogeochemical variation driving aragonite saturation state in West and East Greenland (left). Local variation on a fjord scale is controlled by circulation driven by glacial morphology (LTG vs MTG) (right).

a different up-stream history of the deep water, or increased wind-driven circulation (Dmitrenko, 2015).

Bacterial remineralization of organic matter in deep water can occur at all times of the year. In contrast, the timing of this study in August captures a snapshot of the seasonal influence of primary production on Ω. However, biological activity is not the only driver of Ω in Greenland fjords. Other seasonal boundary conditions including freshwater input drive aragonite undersaturation in coastal Greenland waters.

4.3. Glacial meltwater drives surface corrosive conditions

High freshwater fractions observed in Greenland fjords compared to Svalbard fjords and the Hudson bay illustrate the magnitude of freshwater influence in the region (Azetsu-Scott et al., 2014; Ericson et al., 2019; Fransson et al., 2015; Granskog et al., 2011). Hence, observed TA values reached lower points than in Alaskan & Svalbard fjords, East Siberian sea, Hudson Bay, and the Arctic Ocean highlighting the strong dilution effect of Greenland glacial melt (Anderson et al., 2011; Azetsu-Scott et al., 2014; Evans et al., 2014; Fransson et al., 2015; Yamamoto-Kawai et al., 2009).

Glacial meltwater input strongly impacts the buffer capacity of seawater. As fjords are the gateway between the Greenland Ice Sheet and the open ocean, freshwater plays a dominant role in coastal acidification. An increased sea ice melt and glacial freshwater fraction coincided with aragonite-undersaturation. This mechanism is explained by the low alkalinity and DIC of these freshwater sources (Fig. 4a). Fig. 4c and d shows that sea ice fractions were proportionally low compared to glacial meltwater (though still substantial in eastern fjords) in this time of the season. Sea ice melt has been known to increase surface alkalinity if ikaite ($CaCO_3{\cdot}6H_2O$) is precipitated during freeze up and released when sea ice melts (Rysgaard et al., 2011). When sea ice melt releases this TA to the surface waters, the partial pressure of carbon dioxide (pCO_2) decreases and atmospheric CO_2 uptake increases (Rysgaard et al., 2009). Nevertheless, within our stations sea ice melt was responsible for lowering TA in surface waters relative to DIC (Fig. 4d). Negative sea ice fractions (known as net sea ice formation, Dodd et al., 2012), may also contribute to TA dilution on the west coast or rather reflect uncertainty in our endmember calculations as sea ice formation is unlikely during the month of August. Similarly to sea ice melt, glacial meltwater reduces the saturation state through alkalinity dilution. A linear regression of TA versus salinity of all our carbonate system observations further illustrate the low TA endmembers of glacial meltwater (East: $TA = 465 + 54 \times S$; $R^2 = 0.9$, West: $TA = -24.6 + 66.9 \times S$; $R^2 = 0.88$). Our multi-fjord west coast TA endmember was even lower than in southwest Greenland fjord Nuup Kangerlua as measured by Meire et al. (2015; $TA = 159 + 63 \times S$) and Rysgaard et al. (2012; $TA = 161 + 61 \times S$). Observed TA values reached lower points than in Alaskan & Svalbard fjords, East Siberian sea, Hudson Bay, and the Arctic Ocean highlighting the especially strong dilution effect of Greenland glacial melt (Anderson et al., 2011; Azetsu-Scott et al., 2014; Evans et al., 2014; Fransson et al., 2015; Yamamoto-Kawai et al., 2009). The reduced buffer capacity of glacial-modified water allows CO_2 absorption to have a heightened impact on acidification (Ericson et al., 2019; Evans et al., 2014; Fransson et al., 2015, 2016). These relationships between Ω and glacial freshwater fraction indicate that glacial meltwater runoff is a controlling mechanism of surface water saturation states in coastal Greenland during late summer. Surface aragonite undersaturation is not found in Svalbard fjords however (Cantoni et al., 2020), which may stem from different ice sheet melt rates in the two regions or the larger Atlantic water influence in Svalbard fjords.

In addition to freshwater's dilution impact, glacial and sea ice melt are undersaturated in pCO_2 (Evans et al., 2014) and will contribute to the CO_2 uptake potential of fjord surface waters. Glacial fjords can also exhibit further undersaturation of pCO_2 due to the non-linear effect of salinity on pCO_2 (Meire et al., 2015; Rysgaard et al., 2012). The combined effects of low temperatures, pCO_2 undersaturation, and the non-linear effect of salinity will cause high CO_2 uptake (Sejr et al., 2011), thereby making poorly buffered glacially modified regions of Greenland fjords susceptible to acidification. Accordingly, increased future melting is likely to cause increased acidification.

4.4. Fjord circulation and coastal water masses set baseline corrosive conditions

Circulation of various water masses governs the state of acidification in coastal Greenland as each water mass has a different baseline Ω level (Fig. 7). A crucial factor determining which water mass can enter the fjord is the depth of sills. Deep fjords, e.g. in West Greenland, allow inflow

of dSPMW which is characterized by lower omega values and consequently has a large impact on the carbonate system of fjord bottom water. Additionally, glacier type clearly played a role in the development of corrosive conditions (Table 2). Glacier dynamics greatly impact the estuarine circulation of the fjords (Mortensen et al., 2014). In this study, fjord transects with marine terminating glaciers (MTGs) often saw corrosive conditions develop below the surface layer. Low saturation state values were often seen closer to surface in the inner fjords near the glacial termini (Fig. 7, Supplemental Fig. 2). Wind-driven upwelling of remineralized bottom waters has been observed causing surface omega undersaturation (Mathis et al., 2012). Meanwhile, MTGs drive upwelling of nutrient-rich bottom water in Greenland fjords as subglacial freshwater discharge results in buoyant plumes next to the glacier termini, entraining deeper water (Cape et al., 2019; Meire et al., 2017). This can consequently bring bottom water up to the surface. On the western coast, this brings water from below the aragonite saturation horizon up to shallower depths explaining the presence of shallower corrosive water than in surrounding seas. At the same time, nutrient upwelling from subglacial discharge can also spur phytoplankton blooms which can help to mitigate surface acidification by reducing DIC in the photic zone (Chierici and Fransson, 2009; Meire et al., 2015, 2017; Rysgaard et al., 2012). Nonetheless, later, greater biological production will fuel increased mineralization of bottom waters as dead organic matter sinks below the photic zone.

To the contrary, transects with land terminating glaciers (LTGs) exhibited corrosive conditions within the upper surface layer. Strong thermohaline stratification from glacial river runoff separated this corrosive layer from deeper waters. Warmer fjord surface temperatures likely result from solar warming while in river transport and after surface stratification was established. Increased turbidity and strong stratification from surface runoff could act as a positive feedback mechanism on aragonite undersaturation by limiting primary production and its consumption of surface water CO_2 (Chierici and Fransson, 2009; Ericson et al., 2019; Holding et al., 2019; Middelbo et al., 2018).

Inflow of shelf water into fjord basins can also help explain the observed deep water corrosivity. Undersaturated bottom water seen only on the west coast could be an artifact of the shallower saturation horizon seen in surrounding basins. The aragonite saturation horizon in Baffin Bay and Davis Strait has been observed between 200 and 700 m (Azetsu-Scott et al., 2010; Yamamoto-Kawai et al., 2013). Meanwhile the saturation horizon in the Fram Strait, Greenland Sea and Iceland Sea is observed deeper with depths from 1000 to 4000 m (Fransner et al., 2020; Olafsson et al., 2009). Shallower saturation horizons within Baffin Bay could arise from acidified Arctic Outflow that enters Baffin Bay through the Canadian archipelago (Azetsu-Scott et al., 2010; Yamamoto-Kawai et al., 2013). Meanwhile Greenland and Iceland sea waters are highly influenced by less acidified Atlantic waters. As a result, shelf water inflow into fjords is more likely to be corrosive on the western coast of Greenland due to the shallower saturation horizon.

4.5. Outlook

Here we present the first large scale assessment of the acidification state and carbonate system dynamics in coastal Greenland. Data spanning 6° of latitude and addressing both coastlines provides a more comprehensive description of how Arctic coastal waters respond to a changing climate. Across the Arctic, surface acidification trends have already been observed. Melting sea ice and air-sea CO_2 uptake have driven a decrease in aragonite saturation of up to 0.09 yr^{-1} within surface waters in the Canada basin (Yamamoto-Kawai et al., 2009; Zhang et al., 2020). Meanwhile within the Iceland sea, the decrease in surface Ω of 0.0072 yr^{-1} has been attributed to increases in anthropogenic CO_2 (Olafsson et al., 2009). Modelling anthropogenic emissions scenarios estimates a future drop in pH of between a 0.1–0.4 drop in surface waters (Fransner et al., 2020). As atmospheric concentrations of CO_2 continue to increase in the future, the air-sea exchange will play an increasingly important role in acidification. In Greenland waters, elevated atmospheric CO_2 concentrations will drive uptake of DIC, particularly as delays of seasonal sea ice allow greater time for ocean-atmospheric exchange. Simultaneously, the saturation horizon is becoming shallower. Between 1985 and 2008, the aragonite saturation horizon in the Iceland sea shoaled at a rate of 4 m yr^{-1} (Olafsson et al., 2009). If this trend continues, there is a greater risk that corrosive bottom waters will be shallow enough to spill into east Greenland fjord basins as observed on the west coast.

Under future climate scenarios, glacial meltwater discharge from the Greenland Ice Sheet is expected to increase (Fettweis et al., 2013). As glaciers amplify the seasonal differences in the carbonate system (Cantoni et al., 2020; Evans et al., 2014), increased meltwater input into Greenland fjords will continue to negatively impact shell-forming marine organisms during the summer season. In addition, the synergistic effect of increased freshwater runoff along with heating and greater anthropogenic CO_2 concentrations will further amplify surface acidification (Ericson et al., 2019; Fransson et al., 2016; Hopwood et al., 2020).

Finally, glacial morphology is changing in Greenland with the potential to impact Ω levels. Continued glacial melt and retreat will lead to a transition of some marine-terminating glaciers into land terminating glaciers causing profound implications for Greenland fjords (Howat and Eddy, 2011; Meire et al., 2017). This transition would result in reduced upwelling of nutrient-rich deep water in the melt season (Hopwood et al., 2018). As a result, bottom water with increased DIC concentrations may remain at greater depths within inner fjords. However, new corrosive water will likely be formed as glacial surface runoff strengthens stratification, warms surface waters, and dilutes surface alkalinity. In addition, this transition is likely to reduce summer productivity due to a reduction in nutrient upwelling in addition to light limitation from increased turbidity (Holding et al., 2019; Meire et al., 2017). The uptake of CO_2 by phytoplankton increases the pH of surrounding water, while respiration of CO_2 leads to a reduction in pH (Chierici and Fransson, 2009). Therefore, changes in biological production may also have a large impact on local aragonite saturation. Coastal ecosystems may show resiliency as benthic macroalgae have also been shown to create localized niches of elevated pH that may offer a refuge to marine calcifiers (Krause-Jensen and Duarte, 2014). However, accelerating acidification may still affect the larger ecosystem.

Acidification in Greenlandic fjords is a complex biogeochemical interplay between the atmosphere, seawater, freshwater, and biological systems at various boundaries and depths. This study has successfully captured a large-scale snapshot of August aragonite saturation levels in Greenland fjords and determined the main drivers in the system. However, a greater understanding of the seasonal variation in aragonite saturation is needed to assess the impact of low Ω levels on the biological community. Time series studies aiding the understanding of how these factors and their interactions will change in the future are critical to assess the consequences of ocean acidification in this region.

CRediT authorship contribution statement

Henry Henson: Formal analysis, Data curation, Writing – original draft. **Johnna M. Holding:** Conceptualization, Investigation, Supervision, Funding acquisition, Data curation, Writing – review & editing. **Lorenz Meire:** Investigation, Writing – review & editing. **Søren Rysgaard:** Investigation, Writing – review & editing. **Colin Stedmon:** Investigation, Writing – review & editing. **Alice Stuart-Lee:** Investigation, Writing – review & editing. **Jørgen Bendtsen:** Investigation, Writing – review & editing. **Mikael Sejr:** Conceptualization, Investigation, Supervision, Funding acquisition, Writing – review & editing.

Data availability

Data relevant to reproduce the results of this study have been made available on Zenodo, an all-purpose open research repository created by Open Access Infrastructure for Research in Europe (OPENAire), a project supported by the European Commission, and by CERN, the European Organization for Nuclear Research. Total alkalinity, dissolved inorganic carbon,

and $\delta^{18}O$-H_2O data are available with the following DOI: https://doi.org/10.5281/zenodo.6759882. Environmental variables recorded by CTD instruments are available for cruises from the West and East coasts respectively at the following DOIs: https://doi.org/10.5281/zenodo.4062024 and https://doi.org/10.5281/zenodo.5572329.

Declaration of competing interest

The authors declare that they have no known competing financial interests or personal relationships that could have appeared to influence the work reported in this paper.

Acknowledgements

We thank Kitte Gerlich, Anette Rasmussen, Peter van Breugel for the technical support in the lab and Tinna Christensen for artistic help on our conceptual figure. We thank the captains and crews of RV Sanna and HDMS Lauge Koch, as well as Eik Britsch and Egon Frandsen for logistical support. Cruises were funded by Danish Centre for Marine Science (Grants: 2016-05 and 2017-06). H.H. was supported by the U.S. Fulbright Scholar Program, Danish Government Scholarship Programme, & the Gudrun Gytel Fund as part of his Master's scholarships. J.H. was supported by European Union's Horizon 2020 research and innovation programme under the Marie Sklodowska-Curie grant agreement no. 752325 (GrIS-Melt) and under grant agreement no. 727890 (INTAROS). L.M. was funded by research programme VENI with project number 016.Veni.192.150, which is financed by the Dutch Research Council (NWO). This study is a contribution the project FACE-IT (The Future of Arctic Coastal Ecosystems – Identifying Transitions in Fjord Systems and Adjacent Coastal Areas). FACE-IT has received funding from the European Union's Horizon 2020 research and innovation programme under grant agreement no. 869154.

Appendix. Supplementary data

Supplementary data to this article can be found online at https://doi.org/10.1016/j.scitotenv.2022.158962.

References

Aagaard, K., Coachman, L.K., 1968. The East Greenland Current North of Denmark Strait: Part I. 21(3). Arctic Institute of North America, pp. 181–200. https://doi.org/10.14430/arctic3262.

AMAP, 2018. AMAP Assessment 2018: Arctic Ocean Acidification.

Anderson, L.G., Björk, G., Jutterström, S., Pipko, I., Shakhova, N., Semiletov, I., Wåhlström, I., 2011. East Siberian Sea, an Arctic region of very high biogeochemical activity. Biogeosciences 8 (6), 1745–1754. https://doi.org/10.5194/bg-8-1745-2011.

Arendt, K.E., Nielsen, T., Rysgaard, S., Tönnesson, K., 2010. Differences in plankton community structure along the Godthåbsfjord, from the Greenland ice sheet to offshore waters. Mar. Ecol. Prog. Ser. 401, 49–62. https://doi.org/10.3354/meps08368.

Azetsu-Scott, K., Clarke, A., Falkner, K., Hamilton, J., Jones, E.P., Lee, C., Petrie, B., Prinsenberg, S., Starr, M., Yeats, P., 2010. Calcium carbonate saturation states in the waters of the Canadian Arctic Archipelago and the Labrador Sea. J. Geophys. Res. 115 (C11), C11021. https://doi.org/10.1029/2009JC005917.

Azetsu-Scott, K., Starr, M., Mei, Z.-P., Granskog, M., 2014. Low calcium carbonate saturation state in an Arctic inland sea having large and varying fluvial inputs: the Hudson Bay system. J. Geophys. Res. Oceans 119 (9), 6210–6220. https://doi.org/10.1002/2014JC009948.

Bamber, J.L., Tedstone, A.J., King, M.D., Howat, I.M., Enderlin, E.M., van den Broeke, M.R., Noel, B., 2018. Land ice freshwater budget of the Arctic and North Atlantic oceans: 1. Data, methods, and results. J. Geophys. Res. Oceans 123 (3), 1827–1837. https://doi.org/10.1002/2017JC013605.

Bates, N.R., Garley, R., Frey, K.E., Shake, K.L., Mathis, J.T., 2014. Sea-ice melt CO2–carbonate chemistry in the western Arctic Ocean: meltwater contributions to air–sea CO2; gas exchange, mixed-layer properties and rates of net community production under sea ice. Biogeosciences 11 (23), 6769–6789. https://doi.org/10.5194/bg-11-6769-2014.

Bates, N.R., Mathis, J.T., 2009. The Arctic Ocean marine carbon cycle: evaluation of air-sea CO2 exchanges, ocean acidification impacts and potential feedbacks. Biogeosciences 6, 2433–2459.

Bates, N.R., Mathis, J.T., Cooper, L.W., 2009. Ocean acidification and biologically induced seasonality of carbonate mineral saturation states in the western Arctic Ocean. J. Geophys. Res. 114 (C11), C11007. https://doi.org/10.1029/2008jc004862.

Bednaršek, N., Feely, R.A., Howes, E.L., Hunt, B.P.V., Kessouri, F., León, P., Lischka, S., Maas, A.E., McLaughlin, K., Nezlin, N.P., Sutula, M., Weisberg, S.B., 2019. Systematic review and meta-analysis toward synthesis of thresholds of ocean acidification impacts on calcifying pteropods and interactions with warming. Front. Mar. Sci. 6, 227. https://doi.org/10.3389/fmars.2019.00227.

Bednaršek, N., Tarling, G.A., Bakker, D.C.E., Fielding, S., Jones, E.M., Venables, H.J., Ward, P., Kuzirian, A., Lézé, B., Feely, R.A., Murphy, E.J., 2012. Extensive dissolution of live pteropods in the Southern Ocean. Nat. Geosci. 5 (12), 881–885. https://doi.org/10.1038/ngeo1635.

Bendtsen, J., Mortensen, J., Lennert, K., K. Ehn, J., Boone, W., Galindo, V., Hu, Y., Dmitrenko, I.A., Kirillov, S.A., Kjeldsen, K.K., Kristoffersen, Y., G. Barber, D., Rysgaard, S., 2017. Sea ice breakup and marine melt of a retreating tidewater outlet glacier in northeast Greenland (81°N). Sci. Rep. 7 (1), 4941. https://doi.org/10.1038/s41598-017-05089-3.

Bourke, R.H., Newton, J.L., Paquette, R.G., Tunnicliffe, M.D., 1987. Circulation and water masses of the East Greenland shelf. J. Geophys. Res. 92 (C7), 6729. https://doi.org/10.1029/jc092ic07p06729.

Brown, K.A., Holding, J.M., Carmack, E.C., 2020. Understanding regional and seasonal variability is key to gaining a Pan-Arctic perspective on Arctic Ocean freshening. Front. Mar. Sci. 7, 606. https://doi.org/10.3389/fmars.2020.00606.

Cantoni, C., Hopwood, M.J., Clarke, J.S., Chiggiato, J., Achterberg, E.P., Cozzi, S., 2020. Glacial drivers of marine biogeochemistry indicate a future shift to more corrosive conditions in an Arctic Fjord. J. Geophys. Res. Biogeosci. 125 (11). https://doi.org/10.1029/2020JG005633.

Cape, M.R., Straneo, F., Beaird, N., Bundy, R.M., Charette, M.A., 2019. Nutrient release to oceans from buoyancy-driven upwelling at Greenland tidewater glaciers. Nat. Geosci. 12 (1), 34–39. https://doi.org/10.1038/s41561-018-0268-4.

Carlson, D.F., Holding, J.M., Bendtsen, J., Markager, S., Møller, E.F., Meire, L., Rysgaard, S., Dalsgaard, T., Sejr, M.K., 2020. CTD Profiles From the R/V Sanna Cruise to Northwest Greenland fjords, August 11-31, 2016. https://doi.org/10.5281/zenodo.4062024.

Carlson, D.F., Pasma, J., Jacobsen, M.E., Hansen, M.H., Thomsen, S., 2019. Retrieval of Ice Samples Using the Ice Drone. Front. Earth Sci. 7, 287. https://doi.org/10.3389/feart.2019.00287.

Carmack, Yamamoto-Kawai, M., Haine, T.W.N., Bacon, S., Bluhm, B.A., Lique, C., Melling, H., Polyakov, I.V., Straneo, F., Williams, W.J., Timmermans, M.-L., 2016. Freshwater and its role in the Arctic Marine System: sources, disposition, storage, export, and physical and biogeochemical consequences in the Arctic and global oceans. J. Geophys. Res. Biogeosci. 121 (3), 675–717. https://doi.org/10.1002/2015JG003140.

Chierici, M., Fransson, A., 2009. Calcium carbonate saturation in the surface water of the Arctic Ocean: undersaturation in freshwater influenced shelves. Biogeosciences 6, 2421–2432. https://doi.org/10.5194/bg-6-2421-2009.

Christensen, T.R., Topp-Jørgensen, E., Sejr, M.K., Schmidt, N.M., 2017. Foreword: synthesis of the Greenland ecosystem monitoring program. Ambio 46 (S1), 1–2. https://doi.org/10.1007/s13280-016-0860-z.

Cox, K.A., Stanford, J.D., McVicar, A.J., Rohling, E.J., Heywood, K.J., Bacon, S., Bolshaw, M., Dodd, P.A., De la Rosa, S., Wilkinson, D., 2010. Interannual variability of Arctic Sea ice export into the East Greenland Current. J. Geophys. Res. 115 (C12), C12063. https://doi.org/10.1029/2010JC006227.

Dickson, A.G., Millero, F.J., 1987. A comparison of the equilibrium constants for the dissociation of carbonic acid in seawater media. Deep Sea Res. 34 (10), 1733–1743. https://doi.org/10.1016/0198-0149(87)90021-5.

Dmitrenko, I.A., 2015. Polynya Impacts on Water Properties in a Northeast Greenland Fjord. 8.

Dodd, P.A., Rabe, B., Hansen, E., Falck, E., Mackensen, A., Rohling, E., Stedmon, C., Kristiansen, S., 2012. The freshwater composition of the Fram Strait outflow derived from a decade of tracer measurements: composition of the Fram Strait outflow. J. Geophys. Res. Oceans 117 (C11). https://doi.org/10.1029/2012JC008011 n/a-n/a.

Doney, S.C., Fabry, V.J., Feely, R.A., Kleypas, J.A., 2009. Ocean acidification: the other CO2 problem. Annu. Rev. Mar. Sci. 1 (1), 169–192. https://doi.org/10.1146/annurev.marine.010908.163834.

Ericson, Y., Falck, E., Chierici, M., Fransson, A., Kristiansen, S., 2019. Marine CO2 system variability in a high arctic tidewater-glacier fjord system, Tempelfjorden, Svalbard. Cont. Shelf Res. 181, 1–13. https://doi.org/10.1016/j.csr.2019.04.013.

Evans, W., Mathis, J.T., Cross, J.N., 2014. Calcium carbonate corrosivity in an Alaskan inland sea. Biogeosciences 11 (2), 365–379. https://doi.org/10.5194/bg-11-365-2014.

Feely, R.A., 2004. Impact of anthropogenic CO2 on the CaCO3 system in the oceans. Science 305 (5682), 362–366. https://doi.org/10.1126/science.1097329.

Fettweis, X., Franco, B., Tedesco, M., van Angelen, J.H., Lenaerts, J.T.M., van den Broeke, M.R., Gallée, H., 2013. Estimating the Greenland ice sheet surface mass balance contribution to future sea level rise using the regional atmospheric climate model MAR. Cryosphere 7 (2), 469–489. https://doi.org/10.5194/tc-7-469-2013.

Forryan, A., Bacon, S., Tsubouchi, T., Torres-Valdés, S., Naveira Garabato, A.C., 2019. Arctic freshwater fluxes: sources, tracer budgets and inconsistencies. Cryosphere 13 (8), 2111–2131. https://doi.org/10.5194/tc-13-2111-2019.

Fransner, F., Fröb, F., Tjiputra, J., Chierici, M., Fransson, A., Jeansson, E., Johannessen, T., Jones, E., Lauvset, S.K., Ólafsdóttir, S.R., Omar, A., Skjelvan, I., Olsen, A., 2020. Nordic seas acidification. Biogeochemistry: Open Ocean https://doi.org/10.5194/bg-2020-339.

Fransson, A., Chierici, M., Hop, H., Findlay, H.S., Kristiansen, S., Wold, A., 2016. Late winter-to-summer change in ocean acidification state in Kongsfjorden, with implications for calcifying organisms. Polar Biol. 39 (10), 1841–1857. https://doi.org/10.1007/s00300-016-1955-5.

Fransson, A., Chierici, M., Miller, L.A., Carnat, G., Shadwick, E., Thomas, H., Pineault, S., Papakyriakou, T.N., 2013. Impact of sea-ice processes on the carbonate system and ocean acidification at the ice-water interface of the Amundsen Gulf, Arctic Ocean. J. Geophys. Res. Oceans 118 (12), 7001–7023. https://doi.org/10.1002/2013JC009164.

Fransson, A., Chierici, M., Nomura, D., Granskog, M.A., Kristiansen, S., Martma, T., Nehrke, G., 2015. Effect of glacial drainage water on the CO 2 system and ocean acidification state in an Arctic tidewater-glacier fjord during two contrasting years. J. Geophys. Res. Oceans 120 (4), 2413–2429. https://doi.org/10.1002/2014jc010320.

Fransson, A., Chierici, M., Nomura, D., Granskog, M.A., Kristiansen, S., Martma, T., Nehrke, G., 2020. Influence of glacial water and carbonate minerals on wintertime sea-ice biogeochemistry and the CO2 system in an Arctic fjord in Svalbard. Ann. Glaciol. 61 (83), 320–340. https://doi.org/10.1017/aog.2020.52.

Granskog, M.A., Kuzyk, Z.Z.A., Azetsu-Scott, K., Macdonald, R.W., 2011. Distributions of runoff, sea-ice melt and brine using δ18O and salinity data—a new view on freshwater cycling in Hudson Bay. J. Mar. Syst. 88 (3), 362–374. https://doi.org/10.1016/j.jmarsys.2011.03.011.

Guinotte, J.M., Fabry, V.J., 2008. Ocean acidification and its potential effects on marine ecosystems. Ann. N. Y. Acad. Sci. 1134 (1), 320–342. https://doi.org/10.1196/annals.1439.013.

Holding, J.M., Carlson, D.F., Meire, L., Stuart-Lee, A., Møller, E.F., Markager, S., Lund-Hansen, L., Stedmon, C., Britsch, E., Sejr, M.K., 2021. CTD Profiles From the HDMS Lauge Koch Cruise to East Greenland Fjords, August 2018. https://doi.org/10.5281/zenodo.5572329.

Holding, J.M., Markager, S., Juul-Pedersen, T., Paulsen, M.L., Møller, E.F., Meire, L., Sejr, M.K., 2019. Seasonal and spatial patterns of primary production in a high-latitude fjord affected by Greenland Ice Sheet run-off. Biogeosciences 16 (19), 3777–3792. https://doi.org/10.5194/bg-16-3777-2019.

Hopwood, M.J., Carroll, D., Browning, T.J., Meire, L., Mortensen, J., Krisch, S., Achterberg, E.P., 2018. Non-linear response of summertime marine productivity to increased meltwater discharge around Greenland. Nat. Commun. 9 (1), 3256. https://doi.org/10.1038/s41467-018-05488-8.

Hopwood, M.J., Carroll, D., Dunse, T., Hodson, A., Holding, J.M., Iriarte, J.L., Ribeiro, S., Achterberg, E.P., Cantoni, C., Carlson, D.F., Chierici, M., Clarke, J.S., Cozzi, S., Fransson, A., Juul-Pedersen, T., Winding, M.H.S., Meire, L., 2020. Review article: how does glacier discharge affect marine biogeochemistry and primary production in the Arctic? Cryosphere 14 (4), 1347–1383. https://doi.org/10.5194/tc-14-1347-2020.

Howat, I.M., Eddy, A., 2011. Multi-decadal retreat of Greenland's marine-terminating glaciers. J. Glaciol. 57 (203), 389–396. https://doi.org/10.3189/002214311796905631.

Jones, E.M., Chierici, M., Menze, S., Fransson, A., Ingvaldsen, R.B., Lødemel, H.H., 2021. Ocean acidification state variability of the Atlantic Arctic Ocean around northern Svalbard. Prog. Oceanogr. 199 (102708), 0079–6611. https://doi.org/10.1016/j.pocean.2021.102708.

Key, R.M., Olsen, A., Van Heuven, S., Lauvset, S.K., Velo, A., Lin, X., Schirnick, C., Kozyr, A., Tanhua, T., Hoppema, M., Jutterstrom, S., Steinfeldt, R., Jeansson, E., Ishi, M., Perez, F.F., Suzuki, T., 2015. Global Ocean Data Analysis Project, Version 2 (GLODAPv2), ORNL/CDIAC-162, ND-P093 [Data Set]. Carbon Dioxide Information Analysis Center (CDIAC) https://doi.org/10.3334/CDIAC/OTG.NDP093_GLODAPV2.

Krause-Jensen, D., Duarte, C.M., 2014. Expansion of vegetated coastal ecosystems in the future Arctic. Front. Mar. Sci. 1. https://doi.org/10.3389/fmars.2014.00077.

Krause-Jensen, D., Duarte, C.M., Hendriks, I.E., Meire, L., Blicher, M.E., Marbà, N., Sejr, M.K., 2015. Macroalgae contribute to nested mosaics of pH variability in a subarctic fjord. Biogeosciences 12 (16), 4895–4911. https://doi.org/10.5194/bg-12-4895-2015.

Lavigne, H., Gattuso, J., 2010. Seacarb: Seawater Carbonate Chemistry With R R package version.

Lueker, T.J., Dickson, A.G., Keeling, C.D., 2000. Ocean pCO_2 calculated from dissolved inorganic carbon, alkalinity, and equations for K_1 and K_2: validation based on laboratory measurements of CO_2 in gas and seawater at equilibrium. Mar. Chem. 70 (1–3), 105–119. https://doi.org/10.1016/S0304-4203(00)00022-0.

Mathis, J.T., Cross, J.N., Bates, N.R., 2011. The role of ocean acidification in systemic carbonate mineral suppression in the Bering Sea. Geophys. Res. Lett. 38 (19), n/a-n/a. https://doi.org/10.1029/2011GL048884.

Mathis, J.T., Pickart, R.S., Byrne, R.H., McNeil, C.L., Moore, G.W.K., Juranek, L.W., Liu, X., Ma, J., Easley, R.A., Elliot, M.M., Cross, J.N., Reisdorph, S.C., Bahr, F., Morison, J., Lichendorf, T., Feely, R.A., 2012. Storm-induced upwelling of high pCO2 waters onto the continental shelf of the western Arctic Ocean and implications for carbonate mineral saturation states. Geophys. Res. Lett. 39 (7). https://doi.org/10.1029/2012GL051574 n/a-n/a.

Mehrbach, C., Culberson, C.H., Hawley, J.E., Pytkowicx, R.M., 1973. Measurement of the apparent dissociation constants of carbonic acid in seawater at atmospheric pressure. Limnol. Oceanogr. 18, 897–907. https://doi.org/10.4319/lo.1973.18.6.0897.

Meire, L., Mortensen, J., Meire, P., Juul-Pedersen, T., Sejr, M.K., Rysgaard, S., Nygaard, R., Huybrechts, P., Meysman, F.J.R., 2017. Marine-terminating glaciers sustain high productivity in Greenland fjords. Glob. Chang. Biol. 23 (12), 5344–5357. https://doi.org/10.1111/gcb.13801.

Meire, L., Søgaard, D.H., Mortensen, J., Meysman, F.J.R., Soetaert, K., Arendt, K.E., Juul-Pedersen, T., Blicher, M.E., Rysgaard, S., 2015. Glacial meltwater and primary production are drivers of strong CO2 uptake in fjord and coastal waters adjacent to the Greenland Ice Sheet. Biogeosciences 12 (8), 2347–2363. https://doi.org/10.5194/bg-12-2347-2015.

Middelbo, A.B., Sejr, M.K., Arendt, K.E., Møller, E.F., 2018. Impact of glacial meltwater on spatiotemporal distribution of copepods and their grazing impact in Young Sound NE, Greenland: impact of meltwater on copepod carbon cycling. Limnol. Oceanogr. 63 (1), 322–336. https://doi.org/10.1002/lno.10633.

Mortensen, J., Bendtsen, J., Lennert, K., Rysgaard, S., 2014. Seasonal variability of the circulation system in a West Greenland tidewater outlet glacier fjord, Godthåbsfjord (64°N): Godthåbsfjord. J. Geophys. Res. Earth Surf. 119 (12), 2591–2603. https://doi.org/10.1002/2014JF003267.

Mortensen, J., Lennert, K., Bendtsen, J., Rysgaard, S., 2011. Heat sources for glacial melt in a sub-Arctic fjord (Godthåbsfjord) in contact with the Greenland Ice Sheet. J. Geophys. Res. 116 (C1), C01013. https://doi.org/10.1029/2010JC006528.

Mouginot, J., Rignot, E., Bjørk, A.A., van den Broeke, M., Millan, R., Morlighem, M., Noël, B., Scheuchl, B., Wood, M., 2019. Forty-six years of Greenland Ice Sheet mass balance from 1972 to 2018. Proc. Natl. Acad. Sci. 116 (19), 9239–9244. https://doi.org/10.1073/pnas.1904242116.

Olafsson, J., Olafsdottir, S.R., Benoit-Cattin, A., Danielsen, M., Arnarson, T.S., Takahashi, T., 2009. Rate of Iceland Sea acidification from time series measurements. Biogeosciences 6, 2661–2668.

Qi, D., Wu, Y., Chen, L., Cai, W., Ouyang, Z., Zhang, Y., Anderson, L.G., Feely, R.A., Zhuang, Y., Lin, H., Lei, R., Bi, H., 2022. Rapid acidification of the Arctic Chukchi Sea waters driven by anthropogenic forcing and biological carbon recycling. Geophys. Res. Lett. 49 (4). https://doi.org/10.1029/2021GL097246.

Robbins, L.L., Wynn, J.G., Lisle, J.T., Yates, K.K., Knorr, P.O., Byrne, R.H., Liu, X., Patsavas, M.C., Azetsu-Scott, K., Takahashi, T., 2013. Baseline monitoring of the Western Arctic Ocean estimates 20% of Canadian Basin surface waters are undersaturated with respect to aragonite. PLoS ONE 8 (9), e73796. https://doi.org/10.1371/journal.pone.0073796.

Rysgaard, S., Bendtsen, J., Delille, B., Dieckmann, G.S., Glud, R.N., Kennedy, H., Mortensen, J., Papadimitriou, S., Thomas, D.N., Tison, J.-L., 2011. Sea ice contribution to the air–sea CO2 exchange in the Arctic and Southern Oceans. Tellus B: Chem. Phys. Meteorol. 63 (5), 823–830. https://doi.org/10.1111/j.1600-0889.2011.00571.x.

Rysgaard, S., Bendtsen, J., Pedersen, L.T., Ramløv, H., Glud, R.N., 2009. Increased CO2 uptake due to sea ice growth and decay in the nordic seas. J. Geophys. Res. 114 (C9), C09011. https://doi.org/10.1029/2008JC005088.

Rysgaard, S., Boone, W., Carlson, D., Sejr, M.K., Bendtsen, J., Juul-Pedersen, T., Lund, H., Meire, L., Mortensen, J., 2020. An updated view on water masses on the pan-West Greenland continental shelf and their link to proglacial fjords. J. Geophys. Res. Oceans 125 (2). https://doi.org/10.1029/2019JC015564.

Rysgaard, S., Glud, R.N., Lennert, K., Cooper, M., Halden, N., Leakey, R.J.G., Hawthorne, F.C., Barber, D., 2012. Ikaite crystals in melting sea ice – implications for pCO2 and pH levels in Arctic surface waters. Cryosphere 6 (4), 901–908. https://doi.org/10.5194/tc-6-901-2012.

Sabine, C.L., 2004. The oceanic sink for anthropogenic CO2. Science 305 (5682), 367–371. https://doi.org/10.1126/science.1097403.

Sejr, M.K., Krause-Jensen, D., Rysgaard, S., Sørensen, L.L., Christensen, P.B., Glud, R.N., 2011. Air—Sea flux of CO2 in arctic coastal waters influenced by glacial melt water and sea ice. Tellus Ser. B Chem. Phys. Meteorol. 63 (5), 815–822. https://doi.org/10.1111/j.1600-0889.2011.00540.x.

Steinacher, M., Joos, F., Frölicher, T.L., Plattner, G.-K., Doney, S.C., 2009. Imminent ocean acidification in the Arctic projected with the NCAR global coupled carbon cycle-climate model. Biogeosciences 6 (4), 515–533. https://doi.org/10.5194/bg-6-515-2009.

Sutherland, D.A., Pickart, R.S., Peter Jones, E., Azetsu-Scott, K., Jane Eert, A., Ólafsson, J., 2009. Freshwater composition of the waters off southeast Greenland and their link to the Arctic Ocean. J. Geophys. Res. 114 (C5), C05020. https://doi.org/10.1029/2008JC004808.

Terhaar, J., Kwiatkowski, L., Bopp, L., 2020. Emergent constraint on Arctic Ocean acidification in the twenty-first century. Nature 582 (7812), 379–383. https://doi.org/10.1038/s41586-020-2360-3.

Vernet, M., Ellingsen, I., Marchese, C., Bélanger, S., Cape, M., Slagstad, D., Matrai, P.A., 2021. Spatial variability in rates of net primary production (NPP) and onset of the spring bloom in Greenland shelf waters. Prog. Oceanogr. 198. https://doi.org/10.1016/j.pocean.2021.102655.

Willcox et al., n.d. Willcox, E., …, & Rysgaard, S. (in preparation). In Preparation.

Woosley, R.J., 2021. Evaluation of the temperature dependence of dissociation constants for the marine carbon system using pH and certified reference materials. Mar. Chem. 229, 103914. https://doi.org/10.1016/j.marchem.2020.103914.

Yamamoto-Kawai, M., McLaughlin, F.A., Carmack, E.C., Nishino, S., Shimada, K., 2008. Freshwater budget of the Canada Basin, Arctic Ocean, from salinity, d18O, and nutrients. J. Geophys. Res. 113 (C1), C01007. https://doi.org/10.1029/2006JC003858.

Yamamoto-Kawai, M., McLaughlin, F.A., Carmack, E.C., Nishino, S., Shimada, K., Kurita, N., 2009. Surface freshening of the Canada Basin, 2003–2007: river runoff versus sea ice meltwater. J. Geophys. Res. 114, C00A05. https://doi.org/10.1029/2008jc005000.

Yamamoto-Kawai, M., McLaughlin, F., Carmack, E., 2013. Ocean acidification in the three oceans surrounding northern North America. J. Geophys. Res. Oceans 118 (11), 6274–6284. https://doi.org/10.1002/2013JC009157.

Zhang, Y., Yamamoto-Kawai, M., Williams, W.J., 2020. Two decades of ocean acidification in the surface waters of the Beaufort Gyre, Arctic Ocean: effects of sea ice melt and retreat from 1997–2016. Geophys. Res. Lett. 47 (3). https://doi.org/10.1029/2019GL086421.